The Magnetic Field of the Large Magellanic Cloud Revealed Through Faraday Rotation

B. M. Gaensler,[1,2]* M. Haverkorn,[1] L. Staveley-Smith,[3] J. M. Dickey,[4] N. M. McClure-Griffiths,[3] J. R. Dickel,[5] M. Wolleben[6]

We have measured the Faraday rotation toward a large sample of polarized radio sources behind the Large Magellanic Cloud (LMC) to determine the structure of this galaxy's magnetic field. The magnetic field of the LMC consists of a coherent axisymmetric spiral of field strength ~1 microgauss. Strong fluctuations in the magnetic field are also seen on small (<0.5 parsec) and large (~100 parsecs) scales. The large bursts of recent star formation and supernova activity in the LMC argue against standard dynamo theory, adding to the growing evidence for rapid field amplification in galaxies.

The Milky Way and many other spiral galaxies show well-organized, large-scale magnetic fields (*1*–*3*), whose existence points to a powerful and ubiquitous process that organizes random motions into coherent magnetized structures. The underlying mechanism is believed to be a dynamo, in which magnetic fields are slowly ordered and amplified due to the interplay between turbulence and differential rotation (*4*, *5*). Magnetism in galaxies is usually mapped by observing the orientation of polarized optical and radio emission from the galaxy itself (*3*), but these data have limited spatial resolution (*6*) and can be difficult to interpret (*7*). An alternative is the direct determination of the geometry and strength of magnetic fields, which comes from the Faraday rotation of background radio sources (*8*–*10*), an effect in which birefringence in an intervening magneto-ionized source rotates the plane of linearly polarized radiation. Measurements of background rotation measures (RMs) are free from the difficulties associated with studying polarized emission produced by the source itself, which suffer from a complicated combination of internal and external Faraday rotation, depolarization, and optical extinction.

[1]Harvard-Smithsonian Center for Astrophysics, 60 Garden Street, Mail Stop 6, Cambridge, MA 02138, USA. [2]School of Physics, University of Sydney, New South Wales 2006, Australia. [3]Australia Telescope National Facility, Commonwealth Scientific and Industrial Research Organization, Post Office Box 76, Epping, New South Wales 1710, Australia. [4]Physics Department, University of Tasmania, GPO Box 252-21, Hobart, Tasmania 7001, Australia. [5]Astronomy Department, University of Illinois, 1002 West Green Street, Urbana, IL 61801, USA. [6]Max-Planck-Institut für Radioastronomie, Auf dem Hügel 69, D-53121 Bonn, Germany.

*To whom correspondence should be addressed. E-mail: bgaensler@cfa.harvard.edu

We studied the magnetic field of the Large Magellanic Cloud (LMC) using 1.4-GHz polarization data recorded as part of a hydrogen line survey (*11*) carried out with the Australia Telescope Compact Array (*12*). Over a field of 130 square degrees, we calculated RMs for 291 polarized background sources. Of this sample, about 100 sources lie directly behind the LMC. We used 140 measurements of sources lying outside the LMC to subtract a mean RM, presumably resulting from foreground Faraday rotation in the Milky Way. The resulting distribution of residual Faraday rotation (Fig. 1) shows a strong excess in RM across the extent of the LMC. The implied magnetic field demonstrates spatial coherence: The eastern half of the galaxy shows predominantly positive RMs, and in the west, the RMs are mainly negative.

We converted position on the sky to a location within the LMC disk for each RM measurement, assuming that the galaxy is inclined to the plane of the sky at an angle i = 35°, with its line of nodes at a position angle Θ = 123° (measured north through east) (*13*). The resulting dependence of RM against position angle within the disk of the LMC (Fig. 2) shows a systematic variation, with the maximum mean RM occurring near the line of nodes. These data can be well fit by a cosinusoid of amplitude $\mathrm{RM}_0 = 53 \pm 3$ rad m^{-2}, demonstrating that the coherent component of the LMC's magnetic field has an axisymmetric spiral geometry (*14*), as is seen in other galaxies (*2*, *3*, *14*). The phase of this cosinusoid corresponds to the pitch angle p of the spiral field (*14*), but in this case we can only infer a weak constraint, $|p| \lesssim 20°$, especially given that the uncertainty on Θ is $\gtrsim 10°$ (*13*).

In addition to the coherent field, a structure function analysis indicates random fluctuations in RM, with a standard deviation $\Sigma_{\mathrm{RM}} = 81$ rad m^{-2} and occurring on a characteristic angular scale of ~0.1°, or a length scale $L \sim 90$ pc at the distance to the LMC of 50 kpc. This may represent the evolved supernova remnants (SNRs) and wind bubbles whose interlocking shells dominate the morphology of ionized gas in the LMC on this scale (*15*).

To estimate the relative strength of the ordered and random field components, we assumed that ionized gas in the LMC consists of a disk of projected thickness D, in which cells of linear size L contain clumps of ionized gas of filling factor f and density n_e (*16*). In each cell, the magnetic field is composed of a uniform component of strength B_0 plus a randomly oriented component of strength B_R. If B_R is uncorrelated with fluctuations in n_e, it can be shown that

$$\frac{\Sigma_{\mathrm{RM}}}{|\mathrm{RM}_0|} \approx \left[\frac{L}{2fD}\left(1 + \frac{2}{3}\frac{B_R^2}{B_0^2 \sin^2 i}\right)\right]^{1/2} \quad (1)$$

The occupation length fD of ionized gas is $\mathrm{DM}_0^2/\mathrm{EM}_0 \approx 530$ pc, where $\mathrm{DM}_0 \equiv \int n_e\, dl \approx 100$ cm^{-3} pc and $\mathrm{EM}_0 \equiv \int n_e^2\, dl \approx 19$ pc cm^{-6} are the average dispersion measure (DM) and median extinction-corrected emission measure (EM) integrated through the LMC, respectively (*12*). Equation 1 then implies $B_R/B_0 = 3.6$. The random field dominates the ordered field, as seen in many other galaxies (*2*, *17*).

The actual values of B_0 and B_R can also be estimated. If B_R and fluctuations in n_e are uncorrelated, then the strength of the ordered component of the LMC's magnetic field is

$$B_0 = \frac{|\mathrm{RM}_0|}{K\ \mathrm{DM}_0 \sin i} \approx 1.1\ \mu\mathrm{G} \quad (2)$$

where $K = 0.81$ rad m^{-2} pc^{-1} cm^3 μG^{-1}. The strength of the random field is then $B_R = 3.6B_0 \approx 4.1$ μG, and the total magnetic field strength on large scales is $B_T = (B_0^2 + B_R^2)^{1/2} \approx 4.3$ μG. We note that in selected regions where B and n_e are correlated, as might result from compression in SNR shocks, the above approach overestimates B_0 and underestimates B_R, each by factors of ~2 (*17*).

The polarized background sources are not randomly distributed across the LMC's extent but tend to avoid areas of bright Hα emission (Fig. 1). Specifically, background sources are increasingly depolarized as they propagate through regions of higher EM (Fig. 3). This suggests that we are observing beam depolarization, in which small-scale fluctuations in foreground RM produce interference between polarized rays along adjacent sightlines (*7*). Beam depolarization is only important

when the angular scale of RM fluctuations is smaller than the resolution of the data and the scale of intrinsic polarized structures. Although the resolution here, ~40 arc sec, is comparatively large, extragalactic sources are typically of much smaller angular extent: For 1.4-GHz flux densities in the range 10 to 300 millijanskys (mJy) as observed here, the median angular size is only ~6 arc sec (*18*), or ~1.5 pc when projected against the LMC. The depolarization (Fig. 3) implies strong RM fluctuations on scales $l \ll 1.5$ pc. In such a situation, beam depolarization reduces the intrinsic linearly polarized intensity, P_0, to a level

$$P = P_0 \exp(-2\sigma_{RM}^2 \lambda^4) \quad (3)$$

(*7*, *19*), where λ is the observing wavelength and σ_{RM} is the standard deviation in RMs across the source. To account for the dependence of P/P_0 on EM (Fig. 3), we need to relate σ_{RM} to the EM along a given sightline. If the magnetic field is uncorrelated with the ionized gas density, we expect that $\sigma_{RM} = k\mathrm{EM}^{1/2}$, where k is a constant. With this assumption, the fluctuating magnetic field on a scale of l pc needed to produce the observed depolarization has a strength $B_r \approx k(lK^2/3)^{-1/2}$ μG. In Fig. 3, Eq. 3 has been fit to the data for $P_0 \approx 0.104$ and $k \approx 1.8$ rad m^{-2} pc$^{-1/2}$ cm^3. Assuming $l < 0.5$ pc, we find that $B_r > 5$ μG. We thus infer that there are large RM and magnetic field fluctuations on subparsec scales in the ionized gas of the LMC. This phenomenon is also seen in our own Galaxy and may trace the turbulent winds and H II regions of individual stars (*20*, *21*).

Most spiral galaxies are long-lived systems that exhibit large amounts of rotational shear and that experience relatively constant star formation rates over long periods of time. Coherent magnetic fields in these galaxies are believed to be produced by a dynamo mechanism, in which small-scale turbulent magnetic fields are amplified and ordered by cyclonic motions and differential rotation (*2*, *4*, *5*). However, in galaxies dominated by sudden bursts of star formation and supernova activity, the dramatic injection of energy should disrupt the slow monotonic increase of the large-scale field produced by a standard turbulent dynamo (*22*, *23*). The LMC has experienced several intense bursts of star formation over the past ~4 billion years triggered by repeated close encounters with the Milky Way and with the Small Magellanic Cloud (*24*, *25*) and yet still maintains a coherent spiral magnetic field. Combined with previous results demonstrating the presence of ordered magnetic fields in young galaxies for which the dynamo has had little time to operate (*26*), and in irregular galaxies, which lack large amounts of rotation (*27*), there is now evidence that standard dynamo processes are ineffective in the LMC and these other galaxies. There are several viable alternatives to explain the coherent magnetic fields that we observe. Potentially most pertinent for the LMC is the cosmic ray–driven dynamo, in which recent supernova activity generates a large population of relativistic particles. The buoyancy of these

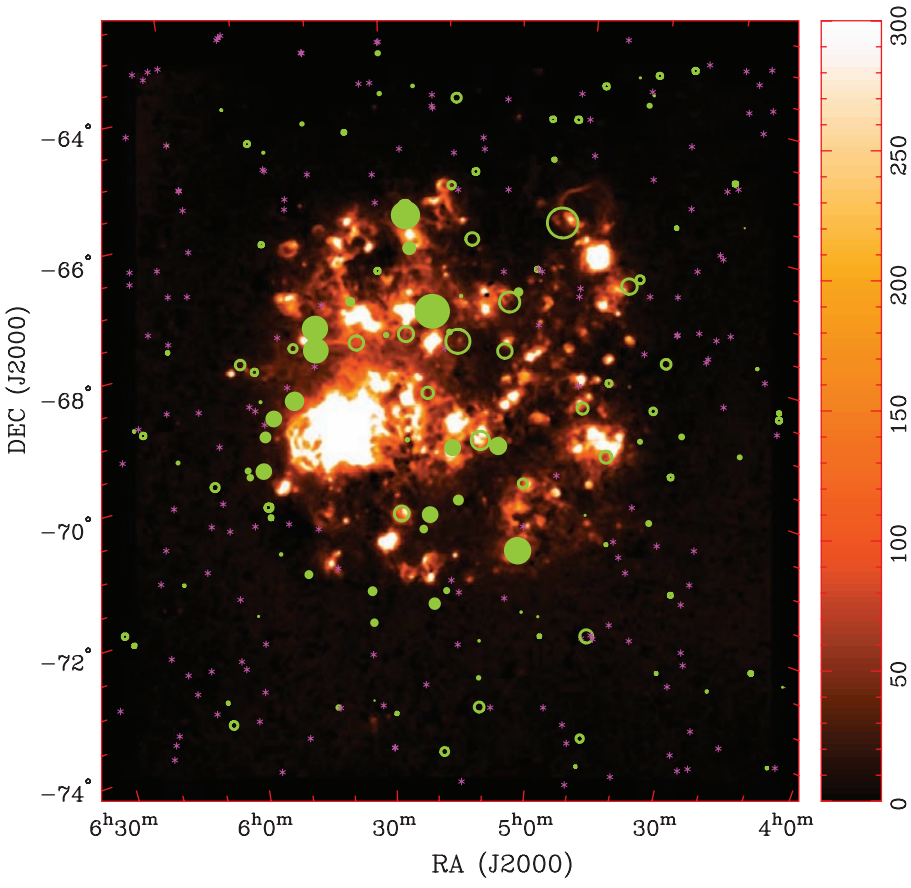

Fig. 1. Faraday rotation measures through the LMC. The image shows the distribution of emission measure toward the LMC in units of pc cm^{-6}, derived from the Southern H-Alpha Sky Survey Atlas (*31*). The symbols show the position, sign, and magnitude of the baseline-subtracted RM measurements (*12*). Solid and open circles (both marked in green) correspond to positive and negative RMs, respectively, and asterisks (marked in purple) indicate RMs that are consistent with zero within their errors. The diameter of each circle is proportional to the magnitude of the RM, the largest positive and negative RMs being +247 ± 13 rad m^{-2} and −215 ± 32 rad m^{-2}, respectively. RA, right ascension; DEC, declination.

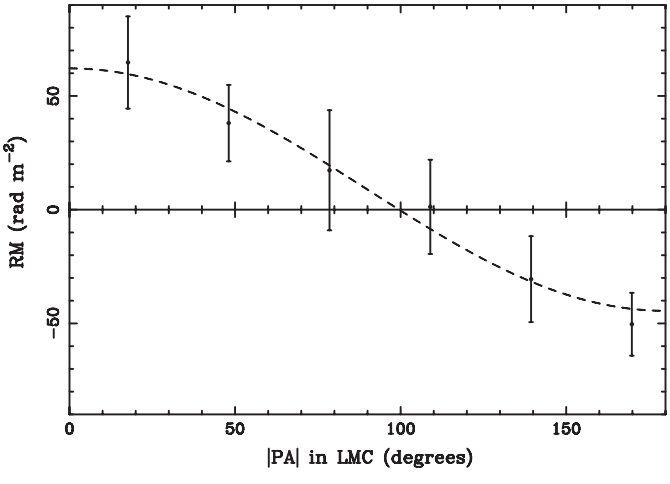

Fig. 2. RM against position angle (PA) within the LMC. The six data points are a binned representation of the 93 RMs that lie within a radius of 3.5° of the center of the EM distribution seen in Fig. 1 [right ascension (J2000) 05^{h}16^{m}03^s, declination (J2000) −68°41′45″], plotted against deprojected position angle within the LMC, measured from the line of nodes. The uncertainty on each datum is the weighted standard error in the mean for RMs in that bin. The dashed line shows a cosinusoidal least-squares fit to the unbinned data, with an amplitude of +53 ± 3 rad m^{-2} and an offset from zero of +9 ± 2 rad m^{-2}. The phase of the cosinusoid is only weakly constrained, falling between ±15°. The fit is not a strong function of the center adopted for the LMC.

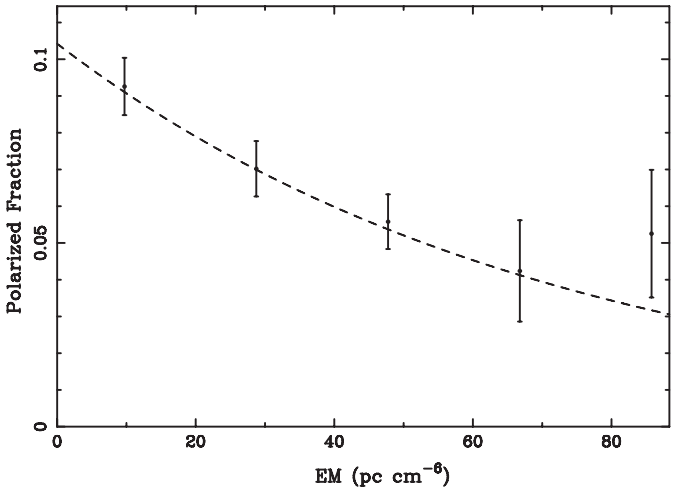

Fig. 3. Polarized fraction of 81 background sources as a function of EM (12 of the 93 sources shown in Fig. 2 have been excluded; six with EM > 100 pc cm^{-6} and six with an observed EM ≤ 0 pc cm^{-6} due to imperfect star subtraction). A Galactic foreground contribution of 3 pc cm^{-6} has been subtracted from each EM measurement. The uncertainty for each binned data point corresponds to the weighted standard error in the mean for each bin. The observed depolarization as a function of EM cannot be a result of source confusion or other observational selection effects because sources with RMs were identified from an image of linear polarization, in which the weak signals from diffuse polarized emission show no correlation with Hα emission. It also cannot be due to excessive Faraday rotation across our observing band (bandwidth depolarization), because for the narrow frequency channels (8 MHz) used here, this effect would manifest itself only for |RM| > 4000 rad m^{-2}, ~20 times the size of any RMs observed. The dashed line shows a least-squares fit of Eq. 3 to the unbinned data, assuming $\sigma_{RM} \propto EM^{1/2}$.

particles inflates magnetic loops out of the disk; adjacent loops reconnect and then are amplified by differential rotation to generate a large-scale spiral field (*28*, *29*). This mechanism not only requires vigorous star formation, as has occurred recently for the LMC, but has a time scale for amplification of only ~0.2 billion years (*29*) and so can quickly generate large-scale magnetic fields before they are dissipated by outflows and tidal interactions. This process can thus potentially account for the coherent fields seen in the LMC and other galaxies (*30*).

References and Notes

1. R. Beck, A. Brandenburg, D. Moss, A. Shukurov, D. Sokoloff, *Annu. Rev. Astron. Astrophys.* **34**, 155 (1996).
2. R. Beck, *Philos. Trans. R. Soc. London Ser. A* **358**, 777 (2000).
3. J.-L. Han, R. Wielebinski, *Chin. J. Astron. Astrophys.* **2**, 293 (2002).
4. A. A. Ruzmaikin, D. D. Sokolov, A. M. Shukurov, *Magnetic Fields of Galaxies* (Kluwer, Dordrecht, Netherlands, 1988).
5. R. M. Kulsrud, *Annu. Rev. Astron. Astrophys.* **37**, 37 (1999).
6. A. Fletcher, E. M. Berkhuijsen, R. Beck, A. Shukurov, *Astron. Astrophys.* **414**, 53 (2004).
7. D. D. Sokoloff *et al.*, *Mon. Not. R. Astron. Soc.* **299**, 189 (1998).
8. J. C. Brown, A. R. Taylor, B. J. Jackel, *Astrophys. J. Suppl.* **145**, 213 (2003).
9. J. L. Han, R. Beck, E. M. Berkhuijsen, *Astron. Astrophys.* **335**, 1117 (1998).
10. B. M. Gaensler, R. Beck, L. Feretti, *N. Astron. Rev.* **48**, 1003 (2004).
11. S. Kim *et al.*, *Astrophys. J.* **503**, 674 (1998).
12. Materials and methods are available as supporting material on *Science* Online.
13. R. P. van der Marel, *The Local Group as an Astrophysical Laboratory,* M. Livio, Ed. (Cambridge Univ. Press, Cambridge, in press) (arxiv.org/abs/astro-/0404192).
14. M. Krause, E. Hummel, R. Beck, *Astron. Astrophys.* **217**, 4 (1989).
15. J. Meaburn, *Mon. Not. R. Astron. Soc.* **192**, 365 (1980).
16. The depolarization demonstrated in Fig. 3 implies that the observed RMs do not probe ionized gas in bright individual H II regions, making this a reasonable assumption.
17. R. Beck, A. Shukurov, D. Sokoloff, R. Wielebinski, *Astron. Astrophys.* **411**, 99 (2003).
18. R. A. Windhorst, E. B. Fomalont, R. B. Partridge, J. D. Lowenthal, *Astrophys. J.* **405**, 498 (1993).
19. B. J. Burn, *Mon. Not. R. Astron. Soc.* **133**, 67 (1966).
20. J. P. Leahy, *Mon. Not. R. Astron. Soc.* **226**, 433 (1987).
21. M. Haverkorn, B. M. Gaensler, N. M. McClure-Griffiths, J. M. Dickey, A. J. Green, *Astrophys. J.* **609**, 776 (2004).
22. P. P. Kronberg, *Rep. Prog. Phys.* **57**, 325 (1994).
23. K. T. Chyży, R. Beck, *Astron. Astrophys.* **417**, 541 (2004).
24. E. W. Olszewski, N. B. Suntzeff, M. Mateo, *Annu. Rev. Astron. Astrophys.* **34**, 511 (1996).
25. K. Bekki, M. Chiba, *Mon. Not. R. Astron. Soc.* **356**, 680 (2005).
26. P. P. Kronberg, J. J. Perry, E. L. H. Zukowski, *Astrophys. J.* **387**, 528 (1992).
27. K. T. Chyży, R. Beck, S. Kohle, U. Klein, M. Urbanik, *Astron. Astrophys.* **355**, 128 (2000).
28. D. Moss, A. Shukurov, D. Sokoloff, *Astron. Astrophys.* **343**, 120 (1999).
29. M. Hanasz, G. Kowal, K. Otmianowska-Mazur, H. Lesch, *Astrophys. J.* **605**, L33 (2004).
30. K. Otmianowska-Mazur, K. T. Chyży, M. Soida, S. von Linden, *Astron. Astrophys.* **359**, 29 (2000).
31. J. E. Gaustad, P. R. McCullough, W. Rosing, D. Van Buren, *Publ. Astron. Soc. Pac.* **113**, 1326 (2001).

32. We thank S. Kim for carrying out the original Australian Telescope Compact Array observations that made this project possible and R. Beck, R. Crutcher, K. Otmianowska-Mazur, D. Elstner, and D. Sokoloff for useful discussions. The Southern H-Alpha Sky Survey Atlas is supported by NSF. The Australia Telescope is funded by the Commonwealth of Australia for operation as a National Facility managed by the Commonwealth Scientific and Industrial Research Organization. Supported by NSF through grant AST-0307358 and by the Denison Fund of the University of Sydney (B.M.G.).

Supporting Online Material

www.sciencemag.org/cgi/content/full/307/5715/1610/DC1
Materials and Methods

17 December 2004; accepted 24 January 2005
10.1126/science.1108832

Molecular Mechanisms for the Functionality of Lubricant Additives

Nicholas J. Mosey,[1] Martin H. Müser,[2]* Tom K. Woo[1]

Wear limits the life-span of many mechanical devices with moving parts. To reduce wear, lubricants are frequently enriched with additives, such as zinc phosphates, that form protective films on rubbing surfaces. Using first-principles molecular dynamics simulations of films derived from commercial additives, we unraveled the molecular origin of how antiwear films can form, function, and dissipate energy. These effects originate from pressure-induced changes in the coordination number of atoms acting as cross-linking agents to form chemically connected networks. The proposed mechanism explains a diverse body of experiments and promises to prove useful in the rational design of antiwear additives that operate on a wider range of surface materials, with reduced environmental side effects.

Whenever two surfaces slide past one another, the potential for the deterioration of one or both of these surfaces exists. Although wear is not necessarily an undesirable effect, such as in manufacturing or polishing, the continuous removal of surface material significantly decreases the usable lifetimes of many devices such as automobile engines (*1*), artificial joints (*2*), and computer hard drives (*3*). The enormous economic and environmental damage due to uncontrolled friction and wear (*4*), as well as the desire to understand the relevant processes, have spurred interdisciplinary research activity

[1]Department of Chemistry, [2]Department of Applied Mathematics, University of Western Ontario, London, Ontario, Canada, N6A 5B7.

*To whom correspondence should be addressed. E-mail: mmuser@uwo.ca